



Energy and Exergy Analysis of a New Power, Heating, Oxygen and Hydrogen Cogeneration Cycle Based on the Sabalan Geothermal Wells

M. Abdolalipouradl*, Sh. Khalilarya, S. Jafarmadar

Department of Engineering, Urmia University, Urmia, Iran

PAPER INFO

Paper history:

Received 01 February 2019

Received in revised form 04 March 2019

Accepted 07 March 2019

Keywords:

Energy and Exergy Analysis

Sabalan Geothermal Power Plant

Organic Rankine Cycle

Hydrogen Production

Heating

ABSTRACT

In this paper, a new power, heating and hydrogen cogeneration cycle from Sabalan geothermal two wells is proposed and analyzed. In the proposed system, a new double flash cycle and organic Rankine cycle are used for power production. A proton exchange membrane (PEM) is also used for hydrogen production and the domestic water heater is used for heating. The impacts of some design parameters, such as separators pressures, evaporator temperature, pinch point temperature difference and PEM temperature on the integrated system performance are investigated and then optimization is done from exergy point of view for three considered scenarios. According to the optimization results, the value of heating, net output power, hydrogen production and thermal and exergy efficiencies of the cogeneration system are obtained as 15751 kW, 18436 kW, 11.13 kg/h, 29.48% and 65.23%, respectively.

doi: 10.5829/ije.2019.32.03c.13

1. INTRODUCTION

Nowadays, the production and use of fossil fuels energy resources or nuclear power plants are associated with environmental pollution and high costs. On the other hand, geothermal energy, in addition to being renewable, has less emissions than the fossil fuels and is one of the clean energies. The advantage of geothermal energy compared to other renewable energy resources (solar and wind) is consistency and reliability [1].

Cogeneration systems are often used for different goals with different resources [2]. Zare [3] compared two tri-generation (heating, cooling and power production) systems for a geothermal source temperature of 120 °C using Organic Rankine Cycle (ORC) and Kalina Cycle (KC). It was shown that the system with KC is more efficient compared to ORC-based one.

Recently, the Proton Exchange Membrane (PEM) has been used more because of its much greater consistency with geothermal sources and the purified

hydrogen production [4, 5]. Gaebi et al. [6] examined a combined cycle with the modified ORC and PEM driven by geothermal energy to produce power and hydrogen. They showed that the energy efficiency is 3.511% and exergy efficiency is 67.58% for R245fa in optimum condition. Yuksel et al. [7] analyzed a novel combined cycle to produce hydrogen, oxygen, cooling, power, heat and hot water by geothermal energy. According to their results, the energy and exergy efficiencies were calculated as 42.59% and 48.24%, respectively. A new configuration to produce electricity, cooling, heating, hot water and hydrogen was investigated by Ratlamwala et al. [8], they reported a daily hydrogen production of 1.85-11.67 kg by increasing geothermal temperature from 440 to 500 K.

The Sabalan geothermal region in northwestern of Iran is one of the under development Geothermal Power Plants (GPP) [9]. Seyedrahimi-Niaq et al. developed a 3D numerical model to simulate the Sabalan GPP wells. To evaluate the subsurface geological condition, three examination wells were drilled in 2002-2004 and two of the wells with different temperatures and pressures were successful [10]. From the thermodynamic and exergoeconomic concepts, single flash and double flash

*Corresponding Author Email: m.abdolalipour@urmia.ac.ir (M. Abdolalipouradl)

with four kinds of ORCs were examined by Bina et al. for Sabalan GPP [11]. Bina et al. [12] analyzed and compared single and double flash for Sabalan GPP and observed that double flash cycle has better performance compared to the single flash while single flash has the lowest total energy cost rate. Aali et al. [13] proposed a new configuration of combined double flash/ORC for the Sabalan geothermal wells using actual data. They indicated that in optimum condition with R141b, exergy efficiency and specific cost of output were calculated as 54.87% and \$4.766/GJ, respectively. For two wells of Sabalan, Abdolalipour et al. [14] examined a new combined two single flash, transcritical CO₂ and ORC to produce power and they showed that the net power, thermal and exergy efficiencies are 19934 kW, 17.05%, 65.38%, respectively. In another study, they used KC 11 instead of ORC and observed that the net output power, thermal and exergy efficiencies increased [15].

Regarding the previous works, it's found that many researches have examined GPP for one well, and it is remarkable that there are few researches which have analyzed the Sabalan GPP for cogeneration goals. In this research, a new cogeneration cycle to produce power, hydrogen, oxygen, heating from two Sabalan wells was investigated. This cogeneration cycle includes a new double flash configuration, PEM, and domestic water heater (DWH). The purposes of this study are multifold and as the following:

- Using different thermodynamic wells from Sabalan GPP as the energy source for cogeneration cycle to produce power, heating, and hydrogen.
- A comprehensive parametric study to investigate the effect of parameters on the performance of the new cycle.
- Optimization of the cogeneration cycle and new double flash/ORC in various scenarios.

2. SYSTEM DESCRIPTION

The schematic diagram of the new cogeneration cycle which uses two wells of Sabalan GPP as the heat source is shown in Figure 1. In the proposed cycle, a new configuration of double flash/ORC for power production, the PEM for hydrogen production, and the DWH for heating are used. The pressure of exhausted saturated liquid from the separator 1 (state 11) reduces in the valve 2 and enters the separator 2. the high-pressure turbine (HPT) exhaust (state 4) is mixed with the saturated vapor coming from the separator 2 (state 13) and produces power in low-pressure turbine (LPT). The saturated liquid from the separator 2 (state 14) is used in ORC for more power production. The ORCT provides the required energy to electrolyzer in PEM for hydrogen production. In short, the PEM system is capable of producing hydrogen and oxygen from the

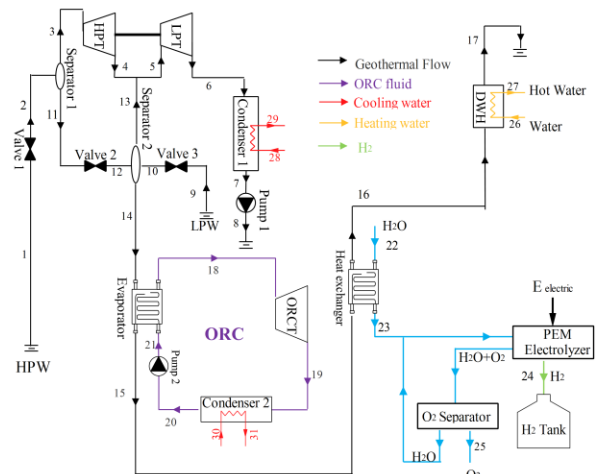


Figure 1. Schematic diagram of the new cogeneration cycle

water while consuming power and heat. The water at the ambient temperature while the geothermal liquid passes through the membrane converter (step 15-16) reaches the electrolyzer temperature, and then the hydrogen exits from the cathode and the mixed flow of water and oxygen exits from the anode in the proton membrane fuel cell. The outgoing hydrogen, which has reached the ambient temperature is stored in a tank to be transferred to the place of consumption. Also, oxygen is separated from the outlet flow of anode by the oxygen separator. Due to the high outlet temperature at point 16, the DWH will be used for heating. The outlet water at point 17 will then be reinjected to the earth wells.

2. 1. PEM Modeling The flow rates of H₂, O₂ and H₂O can be defined as follows [4, 5]:

$$\dot{N}_{\text{H}_2, \text{out}} = \frac{J}{2F} = \dot{N}_{\text{H}_2\text{O, reacted}} \quad (1)$$

$$\dot{N}_{\text{O}_2, \text{out}} = \frac{J}{4F} \quad (2)$$

$$\dot{N}_{\text{H}_2\text{O, out}} = \dot{N}_{\text{H}_2\text{O, in}} - \frac{J}{2F} \quad (3)$$

where F and J are the the Faraday constant and the current density in the PEM system, respectively. The required electricity energy ($\dot{E}_{\text{electric}}$) in the PEM electrolyzer process can be defined as follows [4, 5]:

$$\dot{E}_{\text{electric}} = JV \quad (4)$$

$$V = V_0 + V_{\text{ohm}} + V_{\text{act, c}} + V_{\text{act, a}} \quad (5)$$

where V is the electric potential that is calculated from Equation (5) and V_0 , V_{ohm} , $V_{\text{act, c}}$ and $V_{\text{act, a}}$ are the

reversible potential, the ohmic overpotential, the cathode and anode activation overpotentials, respectively. These four parameters can be calculated by Equations (6-8).

$$V_0 = 1.229 - 0.00085(T_{PEM} - 298) \quad (6)$$

$$V_{ohm} = JR_{PEM} \quad (7)$$

$$V_{act,i} = \frac{RT}{F} \sinh^{-1} \left(\frac{J}{2J_{0,i}} \right) \quad i = a, c \quad (8)$$

where T_{PEM} is the membrane temperature; R_{PEM} is the overall resistance of the system that is calculated through Equations (9-11); $J_{0,i}$ is the exchange current density; and subscripts a and c show anode and cathode, respectively [4, 5].

$$\sigma_{PEM} [\lambda(x)] = [0.5139\lambda(x) - 0.326] \exp \left[1268 \left(\frac{1}{303} - \frac{1}{T} \right) \right] \quad (9)$$

$$\lambda(x) = \frac{\lambda_a - \lambda_c}{D} x + \lambda_c \quad (10)$$

$$R_{PEM} = \int_0^D \frac{dx}{\sigma_{PEM} [\lambda(x)]} \quad (11)$$

where σ_{PEM} , $\lambda(x)$, D , λ_a and λ_c are the local ionic conductivity, the water content at location x in the membrane, the membrane thickness, the water contents at the anode-membrane and the cathode-membrane interface, respectively.

The exchange current density is defined as [4, 5]:

$$J_{0,i} = J_i^{ref} \exp \left(\frac{-E_{act,i}}{RT} \right) \quad , i = a, c \quad (12)$$

where J_i^{ref} and $E_{act,i}$ are the pre-exponential factor and the activation energy for anode and cathode, respectively.

2. 2. Exergy Analysis The total exergy of streams can be obtained as follows [16]:

$$\dot{E}_{tot} = \dot{E}_{ph} + \dot{E}_{ch} \quad (13)$$

where \dot{E}_{ch} is the chemical exergy and \dot{E}_{ph} is the physical exergy that is calculated by Equation (14).

$$\dot{E}_{ph} = \dot{m} (h - h_0 - T_0 (s - s_0)) \quad (14)$$

The exergy destruction of component can be defined as follows [16]:

$$\dot{E}_D = \dot{E}_F - \dot{E}_P \quad (15)$$

where \dot{E}_F is the fuel exergy and \dot{E}_D is the product exergy.

2. 3. Performance of the Cycle The thermal and exergy efficiencies of the new proposed cycle are defined as follows:

$$\eta_{th} = \frac{\dot{W}_{net} + \dot{m}_{H_2} LHV + \dot{Q}_{heating}}{\dot{m}_1 (h_1 - h_0) + \dot{m}_9 (h_9 - h_0)} \quad (16)$$

$$\eta_{ex} = \frac{\dot{W}_{net} + \dot{E}_{24} + \dot{E}_{heating}}{\dot{E}_1 + \dot{E}_9} \quad (17)$$

where,

$$\dot{W}_{net} = \sum \dot{W}_T - (\sum \dot{W}_p + E_{electric}) \quad (18)$$

2. 4. Assumptions

- Pressure drops and heat losses across the pipes and the heat exchangers are not considered.
- R141b is used as the ORC fluid and 50% of the ORC produced power is used in the PEM.
- The ambient pressure and temperature, pinch point difference, PEM temperature, isentropic efficiencies of the pumps and turbines, separators 1 and 2 pressures and evaporator temperature are assumed as 101.3 kPa, 15 °C, 10 °C, 80 °C, 90%, 85%, 900 kPa, 500 kPa and 110 °C, respectively.
- Thermodynamic characteristics of Sabalan GPP wells are given in Table 1 [13].
- The effective parameters in the PEM simulation are shown in Table 2 [4, 5].

TABLE 1. Real data of Sabalan GPP wells

parameter	HPW	LPW
P (kPa)	1072	700
T (°C)	183	165
\dot{m} (kg / s)	57	53
h (kJ / kg)	1150	1100

TABLE 2. Effective parameters in the PEM system

parameter	value	parameter	value
$E_{act,a}$ (kJ / mol)	76	D (µm)	50
$E_{act,c}$ (kJ / mol)	18	F (C / mol)	96486
λ_a	14	J_a^{ref} (A / m ²)	1.7×10^5
λ_c	10	J_c^{ref} (A / m ²)	4.6×10^3

2. 5. Method of Optimization The direct search method is used for optimization by EES from exergy viewpoint in three scenarios as:

- Scenario A: for the double flash/ORC cycle.
- Scenario B: for the double flash/ORC cycle with PEM.
- Scenario C: for the overall cogeneration system.

3. RESULTS AND DISCUSSION

3. 1. Validation The simulated $J-V$ characteristics in the PEM system are compared with the experimental data of Ni, et al. [5] as shown in Figure 2 which shows good accordance with the experimental results. It is found that the V increases rapidly when $J < 200 \text{ A/m}^2$ and it increases steadily with J when $J > 200 \text{ A/m}^2$.

For the assumed condition, the net output power, hydrogen and oxygen production, heating, thermal and exergy efficiencies are calculated for the cycle as 17706 kW, 10.83 kg/h, 85.93 kg/h, 21207 kW, 33.59% and 64.16%, respectively.

3. 2. Parametric Study The influence of the first separator pressure, P_2 , on the performance of the cogeneration cycle is shown in Figure 3, where it's observed that the net output power increases because HPT power generation increases. Also, since the value of hydrogen production and heating are almost constant, the amount of thermal and exergy efficiencies increase continuously with P_2 .

Effect of second separator pressure, P_{10} , on the performance of the cogeneration cycle is illustrated in Figure 4. With increasing P_{10} , LPT and ORCT power generation increase but HPT power generation decreases thus net output power has optimum value. As the $\dot{E}_{\text{electric}}$ increases with ORCT power, the hydrogen production increases as well. When ORCT power generation increases, the value of $\dot{m}_{15}h_{15}$ and $\dot{m}_{16}h_{16}$ and consequently the amount of heating decreases. Thermal efficiency decreases with P_{10} because the decrease of heating dominates $\dot{m}_{H_2}LHV$ and \dot{W}_{net} . Also, the change

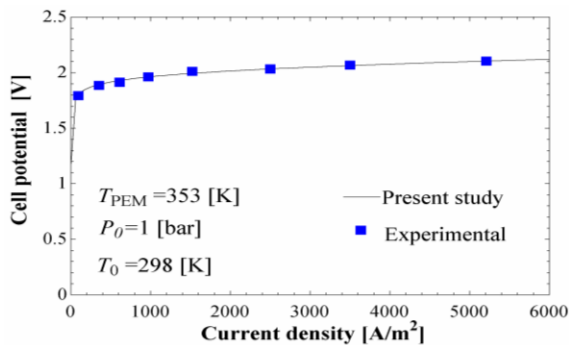


Figure 2. Verification of simulation results for PEM

of exergy of product, heating and hydrogen production leads the exergy efficiency to have an optimum value.

The effect of evaporator temperature, T_{EV} , on the performance of the cycle is depicted in Figure 5. The ORC net power output has an optimum value with T_{EV} , consequently $\dot{E}_{\text{electric}}$ and hydrogen production follows a similar trend with \dot{W}_{net} . When T_{EV} increases, $\dot{m}_{15}h_{15}$. These trends of energy and exergy of products lead the thermal efficiency to increase while the exergy and $\dot{m}_{16}h_{16}$ value and the value of heating increases. Figure 6. With increasing $\Delta T_{pp, EV}$, the ORCT power production and hydrogen production decrease while the efficiency has the maximum value. Variations of the

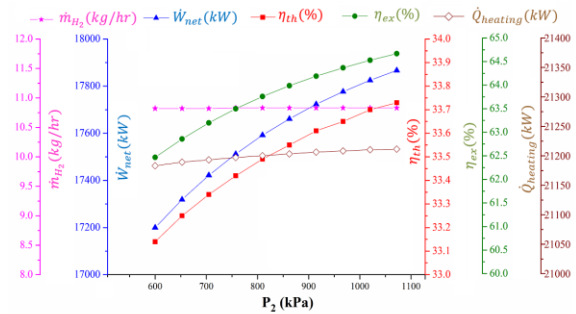


Figure 3. Effect of first separator pressure on the performance of the cogeneration cycle

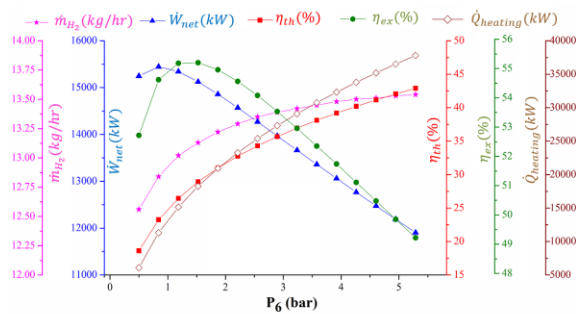


Figure 4. Effect of second separator pressure on the performance of the cogeneration cycle

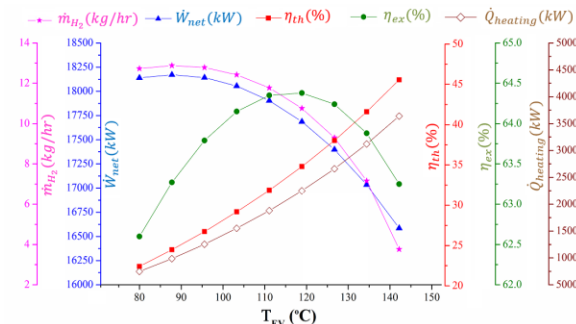


Figure 5. Effect of evaporator temperature on the performance of the cogeneration cycle

five performance parameters with $\Delta T_{PP,EV}$ are shown in heating and thermal efficiencies increase and exergy efficiency decreases with the decrease of exergy production and \dot{E}_{24} .

Figure 7 illustrates the variation of performance of the cogeneration cycle with PEM temperature, T_{PEM} , which indicates that the value of hydrogen production increases but heating decreases because of $m_{16}h_{16}$ reduction with the T_{PEM} . Figure 7 also indicates that the decrease in heating leads to a slight reduction of exergy efficiency. Also, Figure 8 shows that, the greater amount of heating exergy and the produced power lead to the less hydrogen production (about 0.68%). In fact, because the amount of exergy rate for hydrogen production is low due to the very low hydrogen mass flow rate (10.83 kg/h or 0.003 kg/s) compared to the exergy associated with net power and heating production, it leads to small amount of exergy related to hydrogen production.

3. 3. Optimization Result The results of optimization from the exergy point of view for three considered scenarios are outlined in Table 3. Scenario C from thermodynamic and exergic viewpoints has the best performance. In other words, adding PEM and DWH improves performance of new double flash/ORC for Sabalan GPP. Also, Table 3 shows that for the cogeneration Sabalan GPP, the heating, hydrogen

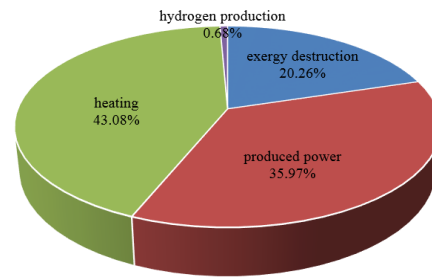


Figure 8. Overall exergy balance of the cogeneration cycle

TABLE 3. Optimization results for various scenarios

Decision variables/Performance parameters	Scenario		
	A	B	C
P_2 (kPa)	1068	1068	1068
P_{10} (kPa)	411.1	411.1	411.1
T_{EV} ($^{\circ}C$)	83.33	83.33	110
$\Delta T_{PP,EV}$ ($^{\circ}C$)	5	5	5
T_{PEM} ($^{\circ}C$)	-	80	80
\dot{W}_{net} (kW)	20131	18442	18346
\dot{m}_{H_2} (kg / hr)	-	11.54	11.13
$\dot{Q}_{heating}$ (kW)	-	-	15751
$\dot{E}_{D,24}$ (kW)	8587	9874	9657
η_h (%)	15.78	16.1	29.48
η_{ex} (%)	60.67	61.94	65.23

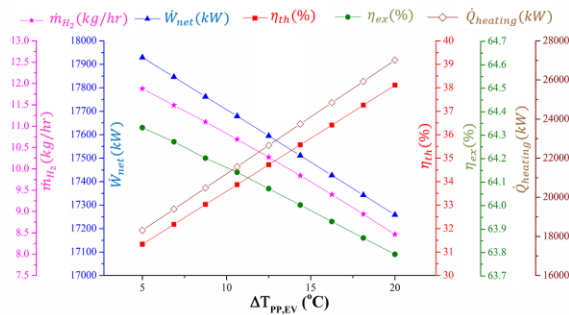


Figure 6. Effect of pinch point temperature difference on the performance of the cogeneration cycle

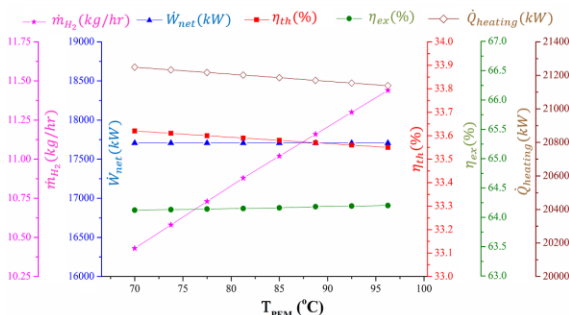


Figure 7. Effect of PEM temperature on the performance of the cogeneration cycle

production, net output power, thermal and exergy efficiencies are determined to be 15751 kW, 11.13 kg/h, 18346 kW, 29.48% and 65.23% at the optimum conditions, respectively.

4. CONCLUSIONS

For heating, power generation and hydrogen production, a new cogeneration cycle from the Sabalan geothermal wells with different pressures and temperatures was proposed and a parametric study as well as an optimization were carried out. Several significant conclusions from the thermodynamic analysis of this study were obtained for the proposed cycle, which include:

- Increasing the first separator pressure leads to increasing the net output power, thermal and exergy efficiencies while the heating and hydrogen production remain almost constant.
- The heating and thermal efficiency decrease with second separator pressure while the net output power and exergy efficiency have optimal values.

- Changes in the net output power, heating and hydrogen production with evaporator temperature lead to an optimal value for exergy efficiency almost in 110 °C.
- The proposed cogeneration system has the best performance from exergy point of view compared to other two considered scenarios.
- In optimization from the exergy viewpoint, heating, hydrogen production, net output power, thermal and exergy efficiencies are calculated to be 15751 kW, 11.13 kg/h, 18346 kW, 29.48% and 65.23%, respectively.

5. REFERENCES

1. Mosaffa, A. H. and Zareei, A., "Proposal and thermoeconomic analysis of geothermal flash binary power plants utilizing different types of organic flash cycle", *Geothermics*, Vol. 72, (2018), 47–63.
2. Jradi, M. and Riffat, S., "Tri-generation systems: Energy policies, prime movers, cooling technologies, configurations and operation strategies", *Renewable and Sustainable Energy Reviews*, Vol. 32, (2014), 396–415.
3. Zare, V., "A comparative thermodynamic analysis of two tri-generation systems utilizing low-grade geothermal energy", *Energy Conversion and Management*, Vol. 118, (2016), 264–274.
4. Pham, A. T., Baba, T., Sugiyama, T., Shudo, T., "Efficient hydrogen production from aqueous methanol in a PEM electrolyzer with porous metal flow field: Influence of PTFE treatment of the anode gas diffusion layer", *International Journal of Hydrogen Energy*, Vol. 38, No. 1, (2013), 73–81.
5. Ni, M., Leung, M. K. H., and Leung, D. Y. C., "Energy and exergy analysis of hydrogen production by a proton exchange membrane (PEM) electrolyzer plant", *Energy Conversion and Management*, Vol. 49, No. 10, (2008), 2748–2756.
6. Ghaebi, H., Farhang, B., Parikhani, T., Rostamzadeh, H., "Energy, exergy and exergoeconomic analysis of a cogeneration system for power and hydrogen production purpose based on TRR method and using low grade geothermal source", *Geothermics*, Vol. 71, (2018), 132–145.
7. Yuksel, Y. E., Ozturk, M., and Dincer, I., "Thermodynamic analysis and assessment of a novel integrated geothermal energy-based system for hydrogen production and storage", *International Journal of Hydrogen Energy*, Vol. 43, No. 9, (2018), 4233–4243.
8. Ratlamwala, T. A. H., Dincer, I., and Gadalla, M. A., "Performance analysis of a novel integrated geothermal-based system for multi-generation applications", *Applied Thermal Engineering*, Vol. 40, (2012), 71–79.
9. Noorollahi, Y., Yousefi, H., Itoi, R., Ehara, S., "Geothermal energy resources and development in Iran", *Renewable and Sustainable Energy Reviews*, Vol. 13, No. 5, (2009), 1127–1132.
10. Noorollahi, Y., Shabbir, M. S., Siddiqi, A. F., Ilyashenko, L. K., Ahmadi, E., "Review of two decade geothermal energy development in Iran, benefits, challenges, and future policy", *Geothermics*, Vol. 77, (2019), 257–266.
11. Mohammadzadeh Bina, S., Jalilinasrabad, S., and Fujii, H., "Thermo-economic evaluation of various bottoming ORCs for geothermal power plant, determination of optimum cycle for Sabalan power plant exhaust", *Geothermics*, Vol. 70, (2017), 181–191.
12. Mohammadzadeh Bina, S., Jalilinasrabad, S., and Fujii, H., "Exergoeconomic analysis and optimization of single and double flash cycles for Sabalan geothermal power plant", *Geothermics*, Vol. 72, (2018), 74–82.
13. Aali, A., Pourmahmoud, N., and Zare, V., "Exergoeconomic analysis and multi-objective optimization of a novel combined flash-binary cycle for Sabalan geothermal power plant in Iran", *Energy Conversion and Management*, Vol. 143, (2017), 377–390.
14. Abdolalipouradl, Mehran, Khalilarya, S., and Jafarmadar, S., "Exergy analysis of a new proposal combined cycle from Sabalan geothermal source", *Modares Mechanical Engineering*, Vol. 18, No. 4, (2018), 11–22.
15. Abdolalipouradl, Mehran, Khalilarya, S., and Jafarmadar, S., "The thermodynamic analysis of a novel integrated transcritical CO₂ with Kalina 11 cycles from Sabalan geothermal wells", *Modares Mechanical Engineering*, Vol. 19, No. 2, (2019), 335–346.
16. Bejan, A., Tsatsaronis, G., Moran, M., Thermal design and optimization, John Wiley & Sons, (1996).

Energy and Exergy Analysis of a New Power, Heating, Oxygen and Hydrogen Cogeneration Cycle Based on the Sabalan Geothermal Wells

M. Abdolalipouradl, Sh. Khalilarya, S. Jafarmadar

Department of Engineering, Urmia University, Urmia, Iran

P A P E R I N F O

چکیده

Paper history:

Received 01 February 2019

Received in revised form 04 March 2019

Accepted 07 March 2019

Keywords:

Energy and Exergy Analysis
Sabalan Geothermal Power Plant
Organic Rankine Cycle
Hydrogen Production
Heating

در این مقاله امکان استفاده از چرخه ترکیبی جدیدی برای تولید همزمان گرمایش، توان و هیدروژن از چاه‌های زمین گرمایی سبلان مورد بررسی قرار گرفته است. در چرخه پیشنهادی، از یک آرایش جدید تبخیر آبی دو مرحله‌ای و چرخه‌ی رانکین آبی به عنوان چرخه مولد توان، از مبدل حرارتی غشای پروتونی برای تولید هیدروژن و از آبگرمکن داخلی برای گرمایش استفاده شده است. چرخه‌ی پیشنهادی سپس نسبت به پارامترهای مهم عملکرد همانند فشار جداساز اول و دوم، دمای اواپراتور، اختلاف دمای نقطه‌ی تنگش و دمای مبدل غشای پروتونی مورد مطالعه قرار گرفته و سپس برای سه سناریوی مختلف از دیدگاه آگزرژی مورد بهینه‌سازی قرار گرفته است. طبق نتایج حاصله در حالت بهینه، برای چرخه‌ی تولید همزمان گرمایش، توان خالص تولیدی، تولید هیدروژن، بازده حرارتی و آگزرژی به ترتیب ۱۵۷۵۱ کیلووات، ۱۸۴۳۶ کیلووات، ۱۱/۱۳ کیلو گرم بر ساعت، ۲۹/۴۸ درصد و ۶۵/۲۳ درصد بدست آمد.

doi: 10.5829/ije.2019.32.03c.13